

ELT Wavefront Control Strategy

Henri Bonnet^a, Jason Spyromilio^a, Christophe Vérinaud^a, Michael Esselborn^a, Enrico Marchetti^a, Miska Le Louarn^a, Steffan Lewis^a, Thomas Pfrommer^a, Fabio Biancat-Marchet^a

^aEuropean Southern Observatory, Garching bei München, Germany

ABSTRACT

The paper gives an overview of the ELT Telescope wavefront control commissioning scenario and synthesizes the functional requirements for the phasing and diagnostic station. A particular attention is given to the problem of pupil fragmentation, a.k.a. petalling and the solution baselined for the SCAO mode of the phasing station is described.

Keywords: segmented mirrors, active optics, adaptive optics

1. INTRODUCTION

The ELT Phasing and Diagnostic Station¹ (PDS), at the Nasmyth platform of the ELT², hosts the sky metrologies for the telescope engineering modes. It is served by the Coudé folding mirror which intercepts the central arcmin of the telescope field of view and feeds it to the PDS for the narrow field characterization, while the field performances are validated with the 3 guide probes at the adapter of the straight through focal station.

The nominal scenario for the wavefront control commissioning of the ELT starts from the conditions delivered at the end of the telescope assembly and is completed when the performance requirements at the interface to the instruments has been demonstrated on sky. This scenario³ was elaborated when the program entered its construction phase and was the baseline for the selection of the equipment in the PDS (Figure 1).

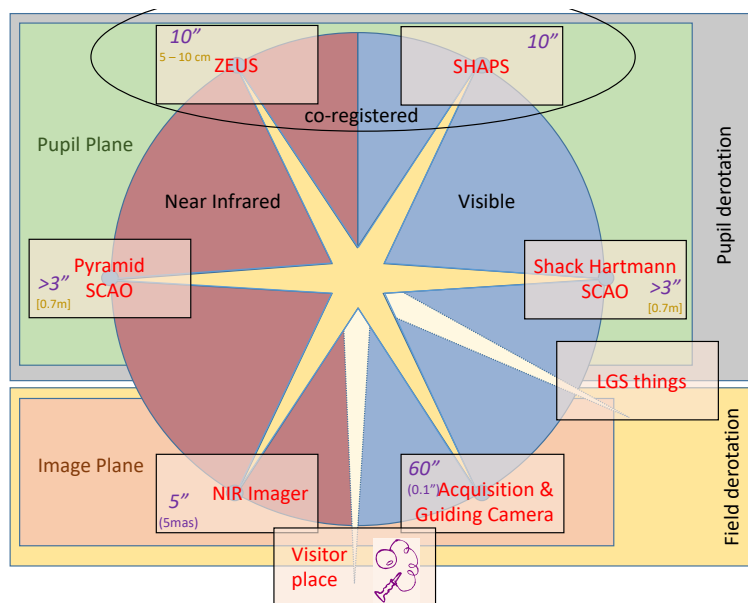


Figure 1. Equipment for the ELT Phasing and Diagnostic station.

A significant driver for the conceptual phase was towards minimizing the complexity of the opto-mechanical assembly while covering the complete commissioning scenario. We distribute the beam to one visible and one infrared port and equip each of them with one focal plane and one pupil plane sensor, i.e. a total of 4 sky-metrologies.

The analysis of the scenario and the identification of its risks finally conducted to a configuration with two additional sensors. The program also provisioned an additional port for the commissioning of the ELT Laser Guide Star Facility as well as the volume for a spare focal plane providing flexibility for incorporating additional steps to the commissioning scenario.

The paper reviews the prominent use cases of the scenario.

2. PRIMARY MIRROR PHASING

The Keck & GTC heritage

The ELT phasing baseline is inherited from the Keck^{4,5} telescope and from GTC⁶ where our wavefront control team had the chance to gain field experience⁷. The ELT SHAPS is a modified Shack-Hartmann sensor. The geometry of the lenslet array matches the segmentation pattern of the ELT primary mirror with shape sub-apertures sampling the surface of the segments to measure the relative tip-tilt errors (stacking) and surface errors (shaping) as well as phasing sub-apertures covering the transitions between adjacent segments.

The phasing sub-apertures are minuscule Fizeau interferometers with two slits, each on a different segment. If the two segments are in the coherence within the optical bandwidth in use, the diffraction pattern of each slit is modulated with fringes at the frequency of the baseline (separation between the two slits) and provides a measurement of the OPD between the two surface elements. This requires that the aperture is operated in the diffraction limited regime and implies that the phasing sub-apertures are not much larger than the coherence scale of the free atmosphere. The ELT phasing sub-apertures are 120 mm edge-to-edge along the normal to the segment edges, allowing the phasing signal to be detected with decent visibility for sub-arcsec seeing conditions across the envisioned optical bandpass.

SHAPS will be equipped with the same suit of color filters as Keck and GTC, with a variety of central wavelengths (650 to 890 nm) and coherence lengths (3 to 100 fringes). Long coherence filters will be used in the early phase of the procedure, the coherencing phase, when the surface discontinuities are in the range of the AIV tolerances, i.e. 100s of microns. They will also support the fast phasing procedure, as we could experience it on sky at the GTC, consisting in measuring the phase through narrow band filters while lifting the 2π ambiguity by using 2 different wavelengths. A complementary method, also demonstrated at the GTC, makes use of a broad band filter (200 nm bandpass centered at 700 nm or 100 nm bandpass centered at 870 nm) and collects phasing measurements across the entire coherence envelope by $\lambda/3$ optical steps. The measurement sequence provides a visibility curve allowing to identify unambiguously the central white fringe and a phase measurement for each step along the sequence.

At GTC, the phase measurements were collected simultaneously with segment shape measurements. In the configuration used by the ESO team, 19 shape sub-apertures per segments measured with high precision the low order figure errors of the segments (focus, astigmatism and trefoil), provided that the integration time was long enough to average out the variations of the free atmosphere seeing. Stable measurements were obtained with a sequence of 27 exposures along an OPD scan length of 9 wavelengths, with 10 seconds integration time at each position, which made the total measurement procedure about 10 minutes, including additional overheads (commanding the segments to the next step, waiting for the stabilization of the primary mirror in its new state, etc...). The resulting dataset provided redundant observability on the surface discontinuities (2 measurement points per edge) and on the segment figure errors. The ensemble was fed to a global reconstruction algorithm which output an estimation of the deviation of the optical surface from its prescription along all measurable parameters (35 relative segment piston, 70 relative tip-tilt of segments and 180 segment shape parameters). The high level of redundancy allowed estimating the measurement noise, rejecting the few 2π phase wrapping errors and rejecting measurement points with outstanding fitting error.

Specific risks in scaling the Keck & GTC baseline to highly segmented telescopes

At ELT, the primary mirror is highly segmented (798 segments) and it is possible to produce surface errors with large amplitude (tens of microns) and low discontinuities at the segment edges. The classical example is the focus mode, completely invisible to the edge sensors measuring the relative translations of adjacent segments along the local normal to the surface. This singularity affects also the Keck and GTC primary mirrors and was lifted in this context with edge sensors specified to be also sensitive to the dihedral angle variations, i.e. the relative tilt of the segments about the axis defined by their common edge. The dihedral sensitivity of the edge sensor baseline for ELT is not a fully controlled design parameters

and it is unclear if the M1 control system will provide a reasonable stability of measurements along this degree of freedom. Beyond the focus mode, the mirror modes with the lowest sensitivity are the two astigmatisms. For these modes, the surface error amplitude scales quadratically with the diameter of the surface. Therefore, the visibility of the mode is inversely proportional to the number of segments and the edge sensors of the ELT primary mirror are 22 times less sensitivity to astigmatism than at the Keck or at the GTC.

In addition to this, the ELT primary is subject to large amplitude dynamic perturbations along its low order modes at various temporal scales. Quasi-statically, the reference provided by the back structure of the mirror deforms by millimeters under the variations of the gravity and thermal loads. The edge sensor would allow compensating exactly these deformations if they were limited to out-of-plane displacements, i.e. to the command space of the segment position actuators (each segment is equipped with 3 axial position actuators providing independent Piston Tip & Tilt actuation relative to the other segments). Unfortunately, the back structure also undergoes substantial in plane deformations, which induces two types of disagreeable effects.

First, the large-scale compression/expansion of the cell modifies the diameter of the primary by a handful of millimeters. The aspherical prescription implies that a segment at the wrong place has the wrong shape. In order to correctly propagate the phase signals in the low order reconstruction of the M1 state, this effect needs to be disentangled from the true figure error of the segments.

Second, the relative displacements of adjacent segments along their common edge (shear mode) or perpendicular to it (gap mode) reaches a maximum amplitude of 200 μ m in the neighbourhood of the Nasmyth platform where the back structure stress is maximum. The capability of the ELT edge sensors to measure not only the piston but also the gap and shear displacements provides in theory full visibility on all deformation modes of the mirror surface, whether in or out of plane, with the exception of the already mentioned focus mode and its in-plane counterpart, consisting of a uniform clocking of all segments around their local normal. Yet, the internal characteristics of the edge sensors and their geometric mounting tolerances induce a coupling of the shear and gap motions towards the piston measurements. Calibrating these coupling coefficients is part of the ELT WFC commissioning plan but the combination of the calibration errors and measurement noise results in a poor capability to track the changes of the M1 figure along its low order modes.

Dynamically, the variable pressure field on the front surface of the ELT primary mirror excites modes with low spatial frequencies, which in turn can be absorbed by the post-focal AO systems both in amplitude (M4 stroke budget) and in reactivity (AO broadband controller bandpass). However, the time scale of the phasing measurements with SHAPS is substantially slower and the optical measurement of the low order terms will be contaminated, unless these aberrations are controlled.

Considering these limitations, the phasing strategy at ELT does not target to bring the primary mirror to its prescription but more modestly to minimize the discontinuities of the surface at the transition between adjacent segments. We take advantage of the adaptive corrector in the telescope optical train to allow the low order figure of M1 to drift under the perturbations listed above. The post focal AO applications will detect the induced aberrations and correct them with M4. The offload process, run as a background task by the telescope control system, transfers the low order quasi-static load from M4 back to M1. We currently envision that about 50 modes, corresponding to a minimum spatial scale of \sim 10 meters in the M1 space, will be controlled in this way.

Amongst them, the telescope will pay a particular attention to the focus and coma terms, which will grow while the secondary mirror moves away from its starting position relative to M1. Correcting these modes at the wrong place, e.g. at M1 result in a residual high order signature induced by the mismatch between the local optical prescription of the segments and the large-scale figure generated by their relative positions on the back structure. This effect, known as scalloping, is a characteristic of the thermo-mechanical properties of the main structure. At the commissioning, we aim to calibrate these effects in the optical model of the telescope used to maintain its alignment against gravitational and thermal perturbations.

The low order variation of the M1 figure also impacts the quality of the phase measurements of SHAPS through two mechanisms. The first one links to the distortions of the image of M1 on the SHAPS lenslet array. Our experience at GTC suggests that a displacement of an edge relative to a phasing sub-aperture along the gap direction starts impacting the phase measurement when the amplitude exceeds 5mm and degrades noticeably the phasing solution for amplitudes larger than 10 mm. We also obtained experimental evidence that these tolerances can probably be moderately relaxed with smart data processing techniques provided that the registration state is monitored with appropriate accuracy. Photometric sub-apertures at the edge of the pupil will provide on-line visibility on the lateral and clocking errors and be corrected by means of a local pupil actuator (lateral control) and K-mirror (clocking control). The phasing and diagnostic station will also

incorporate in its optical design the capacity to adjust the magnification of the pupil image in order to absorb the uncertainty in the delivered f-number (hopefully $\sim 0.5\%$) and relax the PDS manufacturing tolerances. Despite this, the registration of the segmentation pattern with the SHAPS lenslet array is registered as a risk in the ELT WFC.

Risk mitigation

The PDS hosts an alternative phasing sensor, which we currently call ZEUS, after its prototype instantiation in the Active Phasing Experiment^{8,9,10}. ZEUS is a pupil imager with a phase mask in an intermediate focal plane. A field stop transfers an unvignetted field of view of diameter ~ 2 arcsec and the phase mask shifts the central ~ 1 arcsec diameter disk by $\lambda/4$ relative to the field region from 0.5 to 1 arcsec radius. The sensor will operate essentially in H band ($1.65\mu\text{m}$). The 2 arcsec field stop provides spatial filtering controlling the pupil resolution (17cm) and outlines the edges of the segments, whether the phasing is in the coherence length of the filter or not.

In the incoherent regime, the re-imaged pupil is the incoherent superposition of the images of the individual segments. The spatial filtering blurs the images, and the filtering function is such that the incoherent addition of 2 adjacent segments features a depression at the transition between the 2 surfaces. If the OPD between the 2 adjacent segments is within the coherence length of the optical filter, the edge photometry is modulated with the phase of the OPD. The addition of three images, acquired while sampling the OPD space at 3 positions separated by steps of $\lambda/3$, yields an incoherent image of the pupil, with a detectable photometric depression at the location of the segment edges.

This property makes the ZEUS concept suitable to mitigate the risks associated to the poor tolerance of SHAPS to registration errors. The optical operation is performed in the focal plane instead of the pupil plane lenslet array. This eliminates the tight fabrication tolerances of the lenslet array. With the a posteriori allocation of pixels to segment edges, ZEUS is tolerant to any distortion of the pupil image. Moreover, the edges are directly detectable in the phasing data products, while in the case of SHAPS, the monitoring of the registration relies on the indirect signature provided by the photometry in the edge sub-apertures (the true detection of the segment edges in SHAPS is a cumbersome procedure, which requires to put the primary mirror in an incoherent configuration).

The role of the $\lambda/4$ phase shift in the central arcsec is to break the symmetry of the propagation and obtain a signed signature of the OPD in the neighborhood of 0. It also enhanced the sensitivity of ZEUS. Left alone (i.e. with infinite field transmission), this phase shift would reveal in a true discontinuity of the photometric profile across the segment edge transition in the presence of non-zero optical path difference. We believe that a sharp discontinuity, after sampling the signal with pixels of non-zero size, revives the sensitivity of ZEUS to registration errors. The 2 arcsec field stop adapts the effective pupil resolution to the detector sampling and maintains the tolerance to registration errors at the cost of a degraded sensitivity compared to the case of pure phase shift.

Lamentably, ZEUS does not measure the segment figure errors.

The association ZEUS-SHAPS offers the choice between multiple scenarios for the phasing procedure at ELT. Currently we consider for the WFC commissioning a reference scenario, which takes advantage of the known properties of the two sensors. In the initial state, where the uncertainty in the surface steps is large (hundreds of μm), ZEUS will be used in a fast integration mode (10 Hz frame rate or more) while the segments are ramped against one another along an OPD trajectory covering the entire uncertainty range. If the detector integration time is shorter than the wavelength travel time in OPD space, the signal at the edges will be modulated in time while the adjacent segments travel the coherence envelope of the H filter. This reduces the initial phasing error to a few wavelengths, but does not identify the white fringe, because the H band, even in its full extension, is too coherent to perform unambiguously this task.

SHAPS is slower than ZEUS in detecting the coherence during an OPD scan. Yet it can perform this task with its short coherence filter (200 nm bandwidth centered at 700 nm) which has only 3.5 cycles in the first lobe of its coherence envelope. In this regime where the phase does not need to be measured, the tolerance of SHAPS to registration errors is loose. It is therefore a good candidate for the second phase of the procedure consisting in the identification of the white fringe.

The last phase of the procedure, the actual phase measurement, can be performed by either of the two sensors. We also envision combining them to measure the residual segment shape errors (SHAPS) and the phase errors simultaneously. The simultaneity of the two measurements with two sensors relying on different optical operations will consolidate the results in rejecting inconsistent pairs of measurements (phase wrapping errors, local undetermined biases, ...).

Phasing maintenance

Occasional phasing sessions on sky (the baseline is once every two weeks) will update the phasing solution. In the early stages of the ELT, we will need a fast phasing procedure to monitor the stability of the solution and, when needed, update it. A single snapshot in ZEUS is enough to determine statistically the phasing performance and reduce the error of outstanding segments to a small wavelength fraction.

In the maintenance plan, two segments are exchanged per day, which will need to be incorporated in the phasing solution. The ELT primary mirror is aspherical but invariant in its prescription by $\pi/3$ rotation. The 798 segments divide in 133 families of 6 identical segments, one in each of the 6 sectors. A 7th sector will be produced and used as a buffer for the re-coating process. In the learning phase of the program, the newly installed segments will come from the 7th sector, i.e. will not have been exposed to sky prior to their first installation. There are various options to maintain the phasing during this phase.

A metrology device, so called “phasing gun”, is to be installed on a twin version of the segment manipulator, capable of measuring in situ the relative attitude and position of a newly installed segment relative to its (up to) 6 neighbors. This provides a phasing reference for the telescope pointing to zenith, the attitude requested for the segment manipulator operations. An alternative is to run the phasing procedure on sky e.g. during twilight. In both cases, this will provide a reference for a particular attitude, and the uncertainty in the coupling coefficients of the edge sensors with the local gap and shear perturbations will cause a degradation of the phasing performance at other elevation angles. In most cases, the impact will be limited to a few tens of nm but there are outstanding locations in the M1 cell where the relative in-plane motions are large and the impact can exceed 100 nm. The plan is to operate the newly installed segments in the so-called training mode, where their edge sensors are used to maintain their position and attitude relative to their neighbors but are excluded from the global reconstruction of the primary mirror state. The recurrent observation of the phasing error of these segments, e.g. at twilight, will progressively constrain the coupling coefficients and the edge sensors of the new segment will finally be incorporated in the global reconstruction process.

ZEUS was already mentioned as a candidate for the fast phasing procedure needed to execute this plan. We also envision as an alternative the pyramid WFS of the PSF, also capable of measuring the local wavefront steps induced by a phasing error. The pyramid WFS is the baseline WFS for the PDS SCAO mode, used to demonstrate the wavefront performance requirements of the telescope.

3. TELESCOPE ADAPTIVE OPTICS

Sensing baseline

In order to demonstrate the diffraction limitable performance of the beam delivered to the ELT instruments, the phasing and diagnostic station hosts a SCAO wavefront sensor, exposed to the same interface as the science instruments. The baseline selected in phase B is a Shack-Hartmann sensor operated at visible wavelengths.

The ELT wavefront is weakly connected at the transition between the sectors delimited by the spider arms shadows. Standard post focal applications in the first light instrument suite^{11,12,13,14,15} correct the atmospheric turbulence at best at the limit of the spatial frequencies accessible by the M4 adaptive mirror. This represents approximately 4000 modes sampling the SCAO footprint. Taking into account the obscuration by the spider, the 798 segments of M1, with their 1.3m² individual collecting areas form a total collecting area of 988m² and therefore the cutoff spatial scale for a SCAO mode controlling 4000 modes is 0.5 x 0.5 m². Since the width of the spider arm shadow is 0.5m, we may therefore expect that the wavefront information across the shadow can be preserved for SCAO systems operating approximately at the spatial cutoff.

The studies of a Shack-Hartmann based SCAO mode show that, indeed, within the 4000 modes command space, the WFS can theoretically support an exact reconstruction of the incoming wavefront, despite the fragmentation of the pupil into its six sectors. Yet, aliasing with e.g. high spatial orders from the Kolmogorov free atmosphere couple to the command space and the delivered wavefront, with high performance at the scale of each individual sector, features large amplitude optical path differences from sector to sector. At ELT, this is known as the petalling effect, a notion that also covers other sources of petal errors, such as the imperfect propagation of the M1 phasing information under the spider shadows, the phasing errors of the M4 petals or the infamous low wind effect evidenced in the recent years by countless observatories equipped with high performance AO systems.

This limitation of the Shack-Hartmann based SCAO system is owed to the geometric nature of their measurement principle. Various teams¹⁶ have shown that astute wavefront reconstructors, making use of smart priors, can turn around the problem and deliver a high Strehl performance under the fragmented ELT pupil, as long as the telescope wavefront itself starts off petal free and the statistics of the wavefront perturbation spectrum close enough to the standard Kolmogorov model of the free atmosphere. The telescope wavefront sensing has to be able to deal with non-Kolmogorov disturbances and thus we have baselined an alternative phase sensitive SCAO WFS and opted for a pyramid WFS, capable of reconnecting the pupil sectors. We note that in operations the telescope wavefront sensors will not be in the corrected field of view and thus if the systems petals we do not have, at this time, a visibility into petalling.

A drawback of the pyramid is that it has a limited linear range. For this reason, our baseline encompasses two SCAO sensors: SHAO the early Shack-Hartmann baseline and PYR-K a pyramid operated in K band.

The K band was chosen in spite of the induced cryogenics burden because the expected wavefront residual errors (200nm) bring the pyramid sensor close to its linear regime at this wavelength. Simulation at shorter wavelengths suggest at shorter wavelength, it is more difficult to extract the petal signal from the atmospheric residuals¹⁷.

We retain the SHAO to maintain a large dynamic and linear range, which nicely complements PYR-K. We use it in the early phase of the phasing procedure, when the wavefront has not reached a sufficient level of coherence to operate safely with PYR-K. Running a modest SCAO mode, limited in both temporal and spatial bandwidths, rejects the quasi-static low order aberrations arising not only from the free atmosphere but also from the dynamic of the M1 front surface. It is critical to average out, within a decently short integration time, the local wavefront tilt at the location of the SHAPS phasing sub-apertures (nothing resembles more the signal generated by a phasing sub-aperture exposed to a small OPD step than a local wavefront tilt). This SHAO based SCAO will also assist in keeping the beam centered to the phase mask at the intermediate focal plane of ZEUS.

Wavefront reconstruction and controller

The reconstruction of the wavefront, including the petal errors, with a pyramid sensor has been studied by Obereder et al.¹⁸ who first proposed a solution to the problem. At ELT, we prototyped a wavefront reconstructor, which controls explicitly the petalling, in a context that also allows taking care of other sources of control errors, such as the mis-registration between the wavefront sensor and the wavefront corrector (M4).

Our solution is based on a redundant interaction matrix built as a concatenation of modes of the M4 geometric matrix on one hand and the 5 independent petal modes on the other hand. The geometric matrix is the one suggested by the MICADO baseline¹⁹. This is a square matrix with one line/column per actuator in the wavefront corrector. The elements of the matrix are the $5/3^{\text{rd}}$ power of the distance between pairs of actuators. The modes of this matrix form, from a subjectively esthetic point of view, a basis of modes nicely ordered spatially. We tried alternate approaches e.g. the Karhunen-Loève modes of the aperture or the elastic modes of the M4 petals complemented by continuity constraints at the petal edges, but failed to reach the esthetic criterion, i.e. found amongst the group of mid-spatial frequency modes, outstanding modes featuring local waffle patterns along the petal edges. Although vaguely defined, the esthetic criterion reflects substantial differences in the stability of the control loop observed in simulations.

Since the interaction matrix is redundant, we need to define rules for its inversion in order to build a control matrix. We use modal weights proportional to the square root of the eigen values of the geometric matrix (which, thanks of the $5/3^{\text{rd}}$ power, resemble the diagonal of the covariance matrix of the Zernike basis of a filled circular aperture under a Kolmogorov statistics) and assign to the petal modes the same weights as received by the tip and tilt modes. On the output side of the matrix, the coefficients are recombined in Fourier space. This operation is defined in the framework of a linearized pyramid model operated without tip-tilt modulation. Fourier coefficients are given a weight approximately proportional to the inverse of their spatial scale (the approximation is in the addition of a constant to avoid the divergence at the origin of the Fourier space). The weighted interaction matrix is decomposed into its singular modes and the first 3000 modes are selected to form the control matrix.

Our temporal controller is based on a full matrix-vector multiplication to reach the modal space where a standard integral controller is applied. We also use control features borrowed from other projects: the modal gains are updated with the CLOSE algorithm^{20,21} and a leak integrator with gain increasing with the spatial order is applied²².

With this controller, our simulations predict a residual wavefront error of ~ 170 nm rms (Strehl ratio = 79% at $\lambda = 2.2\mu\text{m}$) with nearly imperceptible petal errors (telescope at prescription, bright guide star, seeing = 0.85 arcsec at zenith, zenith

distance = 30 deg, wind speed = 11 m/s, loop rate = 500Hz, loop delay = 2 frames in addition to the frame delay of the wavefront sensor DIT and DM sample and hold).

Petal kick

This performance is reached in steady state after the convergence of the controller. The entrance conditions are those of the free atmosphere, i.e. several microns of wavefront error, by far beyond the linear regime of the wavefront sensor. In addition to this, although the modal gain compensation is modest in K band under the reference Armazones seeing, the control gains in the convergence phase are out of tune, which contributes to slowing down the convergence. For the modes of the geometric matrix, the signal saturates and couples with other modes but the sign remains correct over a large dynamic (± 3 wavelengths). For the petal modes, the response of the pyramid is exactly sinusoidal with the amplitude. This reduces the linear range to not much. Numerical experiments show that the sign of the error signal may even become occasionally wrong during the convergence phase. This results in a petal wise flat wavefront with 2π phase steps between petals.

At ELT, we target a quality of phasing of the M4 petals much smaller than the K band wavelength. Observing the state of M4 and try deriving from it the 2π petal errors is doable at this wavelength in the ideal conditions of our simulations. Yet, we found that the extraction of the petal errors was easier and more robust when based on the integral of the wavefront correction command along the petal modes (which come explicitly as the first modes of the interaction matrix decomposition with little contamination from other things, thanks to the heavy weight given to the petal modes).

The SCAO controller is complemented with a module which monitors the petal integral, applies a low pass filter to reject the noise, and occasionally commands a petal kick to M4 to reject the 2π errors. In all our simulations, including those with large registration errors (see below) and low stellar flux, the petal controller converges to the right solution after less than 0.5 seconds.

Registration control

At ELT, the opto-mechanical distance from M4 to the PDS pyramid wavefront sensor is long. It is therefore likely that the initial alignment state of the M4 image at the entrance pupil of PYR-K will not meet the canonic $1/10^{\text{th}}$ of a sub-aperture tolerance. Moreover, M4, the wavefront corrector, is not conjugated to the telescope pupil and, therefore, controlling the registration to the pupil and to the wavefront corrector are two different tasks. Inspired by the MICADO baseline, we opted for keeping PYR-K optically registered to the pupil. The error signal will be the photometric signal in the 4 pupil images of the detector. At loop closure, when PYR-K is not in its linear range, this signal will be perturbed, which may also contaminate the registration to M4. After convergence of the photometric loop, the residual M4 mis-registration will be the combination of the internal flexures in the telescope main structure and of field effects (PYR-K is supposed to operate on-axis, but at ELT, the notion of optical axis is not quite clearly defined other than by the centering of the M1 footprint on M4). The dominant effect is expected to be the internal flexure in the telescope, which, according to the main structure finite element model would not exceed 10 mm of lateral displacement of M4, i.e. 180 mm of lateral registration error in the entrance pupil space. The WFC commissioning will encompass the task of calibrating this and deliver a blind model for the main structure with substantially better co-registration of M1 and M4.

We expect that the mis-registration at loop closure will be small enough to allow the loop to close but not to avoid the development of waffle modes at the cost of performance and M4 saturations. We therefore need to monitor and compensate on-line the M4 registration error.

Heritier et al.²³ propose to extract an estimation of the registration error from the analysis of the interaction matrix derived from the on line loop products. We propose an equivalent approach formulated in the Fourier space, where the signature can be extracted from a sparse covariance matrix. In Fourier space, a lateral registration error is a phase shift of the Fourier coefficients with amplitude proportional to their position in the UV plane. This allows building a simple registration control strategy: the autocorrelation of the observed Fourier residual are accumulated at the time scale of the loop latency. After 100 ms of integration, the phases of the autocorrelations are fitted to a linear function of the Fourier plane positions and the coefficients of the linear fit used as an indicator of the residual lateral registration error.

The compensation of the registration error is done by applying at each AO cycle the appropriate phase shift. In our simulations, this operation is explicitly executed in Fourier space. Yet, since this process is linear, it can also be incorporated in the control matrix. This is a matter of implementation, beyond the scope of the WFC activity.

Our simulations suggest that this registration control strategy keeps the performance of the system with less than 10% loss in Strehl ratio, while the lateral error of M4 is at its worst pre-commissioning case (10 mm). This is observed both in the bright and faint guide star regime. The petal control also remains stable in these circumstances.

The registration control should also encompass, as a minimum, the control of the clocking error. There, the estimator cannot be limited to observing the autocorrelation function of the Fourier coefficients, because the signature of a rotation in the direct space is also a rotation in the Fourier space and, therefore, the indicator should be based on the observation of the cross-correlation between coefficients of different spatial scale. We have not yet described an estimator, but we believe that this should be doable with a sparse algorithm limited to observing the cross-correlation between adjacent coefficients. If needed, the same approach could also be used to monitor the variations of the M4 image magnification.

The compensation of the M4 clocking error will be done at the K-mirror of the phasing station.

4. CONCLUSIONS

The Phasing and Diagnostic Station is now in its detailed design phase. Meanwhile the Minuscule ELT test bench²⁴ is currently in the last steps of its pre-alignment phase in the laboratory at the ESO Headquarter. In this environment, we will deploy in full the telescope control system. MELT will also be a place where the commissioning scenario will be evaluated and detailed. This establishes a context for the ELT WFC team to further develop the wavefront plan and address in details questions such as, for example, the calibration of the edge sensor coupling coefficients, the transition from the guide probe based wavefront control at telescope preset (~50 controlled modes) to the post focal adaptive optics mode or the on-line diagnostics of the telescope control system.

REFERENCES

- [1] Lewis, S. A. E., et al., "Extremely Large Telescope Prefocal Station A system concept", Proc. SPIE 10700, Ground-based and Airborne Telescopes VII, 107001B (9 July 2018); <https://doi.org/10.1117/12.2313535>
- [2] Cirasuolo, M., "The ESO Extremely Large Telescope", in these proceedings
- [3] Bonnet, H., et al., "Adaptive optics at the ESO ELT", Proc. SPIE 10703, Adaptive Optics Systems VI, 1070310 (10 July 2018); <https://doi.org/10.1117/12.2312407>
- [4] Chanan, G., et al., "Phasing the Mirror Segments of the Keck Telescopes: The Broadband Phasing Algorithm," Appl. Opt. 37, 140-155 (1998) [10.1364/AO.37.000140](https://doi.org/10.1364/AO.37.000140)
- [5] Chanan, G., Ohara, C. and Troy, M., "Phasing the Mirror Segments of the Keck Telescopes II: The Narrow-band Phasing Algorithm," Appl. Opt. 39, 4706-4714 (2000) [10.1364/AO.39.004706](https://doi.org/10.1364/AO.39.004706)
- [6] Álvarez, P., et al., "The GTC project: from commissioning to regular science operation. Current performance and first science results", Proc. SPIE 7733, Ground-based and Airborne Telescopes III, 773305 (July 28, 2010); [10.1117/12.857372](https://doi.org/10.1117/12.857372)
- [7] Bonnet, H., et al., "Fast optical re-phasing of segmented primary mirrors", Proc. SPIE 9145, Ground-based and Airborne Telescopes V, 91451U (22 July 2014); <https://doi.org/10.1117/12.2057457>
- [8] Dohlen, Kjetil, "Phase Masks in Astronomy: from the Mach-Zehnder Interferometer to Coronagraphs", Astronomy with High Contrast Imaging II, Editors : C. Aime and R. Soummer EAS Publication Series, 12 (2004) 33-44
- [9] Vigan, Arthur; Dohlen, Kjetil; Mazzanti, Silvio, "On-sky multiwavelength phasing of segmented telescopes with the Zernike phase contrast sensor," Applied Optics, vol. 50, issue 17, p. 2708 (2011)
- [10] Surdej, I., Yaitskova, N. and Gontje, F., "On-sky performance of the Zernike phase contrast sensor for the phasing of segmented telescopes", Applied Optics Vol. 49, Issue 21, pp. 4052-4062 (2010) <https://doi.org/10.1364/AO.49.004052>
- [11] Neichel, B., et al., "HARMONI at the diffraction limit: From Single Conjugate to Laser Tomography Adaptive Optics", in these proceedings
- [12] Busoni, L., et al., "Adaptive Optics design status of MAORY, the MCAO system of European ELT", in these proceedings
- [13] Bertram, T., et al., "Single Conjugate Adaptive Optics for METIS", in these proceedings
- [14] Vidal, F., et al., "Analysis of the MICADO-MAORY SCAO performance", in these proceedings

- [15] Sauvage, J.-F., et al., "The SCAO module for HARMONI, towards final design", in these proceedings
- [16] Sylvain Bonnefond, et al., "Wavefront reconstruction with pupil fragmentation: study of a simple case", Proc. SPIE 9909, Adaptive Optics Systems V, 990972 (27 July 2016); <https://doi.org/10.1117/12.2234034>
- [17] Bertrou-Cantou, A., et al., "Analysis of the Island effect for MICA0 MAORY SCAO mode", in these proceedings
- [18] Obereder, A., et al., "Dealing with spiders on ELTs: using a Pyramid WFS to overcome residual piston effects", Proc. SPIE 10703, Adaptive Optics Systems VI, 107031D (10 July 2018); <https://doi.org/10.1117/12.2313419>
- [19] Gendron, E., Private communication, 2019
- [20] Déo, V., et al., "Forward with self-adaptive optical gain modal compensation, comparative simulations with various PWFS-class sensors", in these proceedings
- [21] Gendron, E., et al., "Another path for getting ELT-scale pyramid WFS under control?", in these proceedings
- [22] Agapito, G., "Elephants, goldfishes and SOUL: a dissertation on forgetfulness and control systems", in these proceedings
- [23] Heritier, C., et al., "How to deal with Mis-Registrations on ELT with Pyramid WFS?"
- [24] Pfrommer, T. et al., "The Minuscule Extremely Large Telescope (MELT) for Wavefront Control, Phasing and Telescope Control validation – Design and First Results", these proceedings, POSTER-WAV-REC-184